

# Untethered Helmet Mounted functional Near Infrared (fNIR) Biomedical Imaging?

K. Manseta, A.M. Khwaja, E. Sultan, P. Daruwalla, K. Pourrezaei<sup>+</sup>, L. Najafizadeh\*,  
A. Gandjbakhche\*, A.S. Daryoush

Department of ECE, Drexel University, Philadelphia, PA USA 19104

<sup>+</sup>School of Biomedical Engineering and Health Systems, Drexel University, Philadelphia, PA USA 19104

\*National Institutes of Health, 9000 Rockville Pike, Bethesda, MD USA 20892

daryoush@coe.drexel.edu

**Abstract**— Broadband (30-1000MHz) frequency modulated spectroscopic measurements of brain tissue using near IR wavelengths are used for accurate extraction of absorption and scattering coefficients of cortex, CSF, and skull. Design of a helmet mounted untethered functional near IR system is presented in this paper that provides wireless communication between the monitoring and helmet mounted fNIR imaging sensors using high speed wireless ISM band Transmitter and UWB communication standards. Design specifications and predicted performance requirements are presented of the custom designed low power consuming optical transceivers and wireless communication subsystems using IBM 90nm CMOS foundry parameters.

**Index Terms** — Near IR Imaging, Brain Tissue Parameters, UWB Communications, Optical Transceiver, CMOS.

## I. INTRODUCTION

Diffused photon near IR (DPNIR) is a non-invasive optical technique that employs near-infrared (NIR) light to quantitatively characterize the optical properties of various tissues. Quantitative DPNIR methods employing time- or frequency-domain photon migration technologies have only recently been used for breast, brain, wound healing, and pain assessment [1]. This broadband system gives information about the functionality of various parts of brain through measurements of optical absorption and scattering properties to form functional images of brain as functional NIR (fNIR). Better understanding of the brain functionality is tied to better assessment of *Action Potentials* that propagate through neurons to control the voluntary human functions. These action potentials are generated by absorbing blood oxygen as it is circulated into the brain. Knowing the rate of oxygenated and deoxygenated blood circulation will lead to knowledge of brain functionality. Spectroscopic studies of tissue have shown absorption and scattering sensitivity of water, oxygenated, and de-oxygenated hemoglobin at different wavelengths. Therefore, any disorder in functionality of the neurons is then registered [2] as changes in the absorption of oxygenated and de-oxygenated hemoglobin. Commercial fiber based fNIR systems [3] are tethered and not field deployable. Moreover, the systems are designed based on unmodulated (CW) or narrow band (single frequency)

operation and higher tissue parameter extraction accuracy has been demonstrated in broadband frequency modulated systems [4].

This paper presents design and realization challenges of a broadband fNIR system for functional brain imaging. This novel design does not suffer from imaging inaccuracy of narrowband frequency modulated systems and field deployment restrictions of fiberoptic based systems. Design specifications meeting low power consumption are presented in a helmet mounted system that is practical for real time monitoring of head and traumatic brain injury (TBI).

## II. SYSTEM ARCHITECTURE

There are two ways of implementing an fNIR imaging system. Our approach is to use free space optics and wireless communications of collected data as opposed to tethered connection to helmet mounted electronics. Fig. 1 depicts the proposed wireless communication between remote monitoring and helmet mounted fNIR brain imaging system.

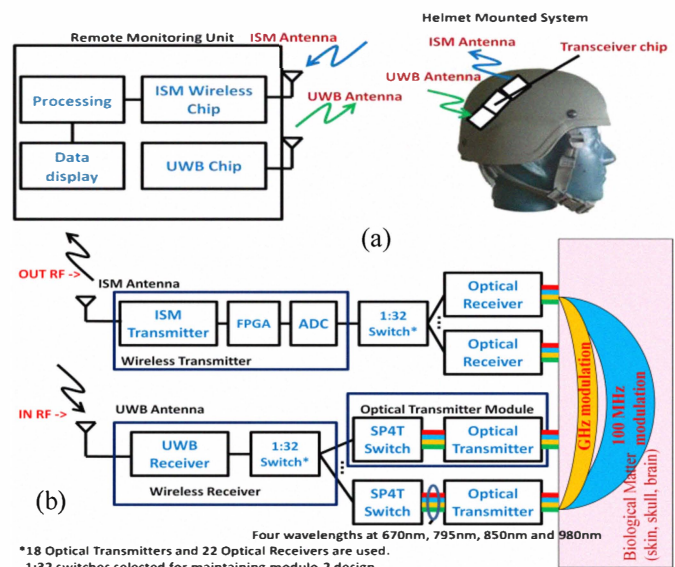


Fig. 1 a) Block diagram of untethered free-space fNIR brain imaging system in wireless communication with remote monitoring; b) details of custom wireless and optical transceivers on the helmet mounted fNIR brain imaging.

Broadband signal of 30-1000MHz covering UWB frequencies of 4.5-5.5GHz is received using the wireless receiver and used for direct modulation of as many as 18 TO-39 can optical transmitters. Four wavelengths of 650nm, 780nm, 850nm, and 980nm are used for measurements of amplitude and phase of backscattered DPNIR waves using 22 optical receivers mounted in ferrules. Separations of optical sources and optical detectors are from 1cm up to 5 cm. At the optical receiver, the scattered light from tissue is collected using small profile GRIN lens [5]. The transmitter module consists of laser driver and low loss SP4T switch to switch between lasers at four different wavelengths as shown in Fig. 2. The optical receiver consists of a PIN photodiode integrated with a trans-impedance amplifier (TZA) to provide required gain without excess noise and high voltage requirements of APD. The optical link output is processed using an FPGA by a time averaging of up to 1000 data points that are frequency averaged data of collected 50 frequency data points of about 1 MHz step each over 50MHz bandwidth [6]. A raw data of 50Mb/s are generated using 16 differential phase bits and 24 differential amplitude bits. The required 50 MHz bandwidth is transmitted using IEEE 802.15.n/ISM band transmitter standard at 2.4GHz.

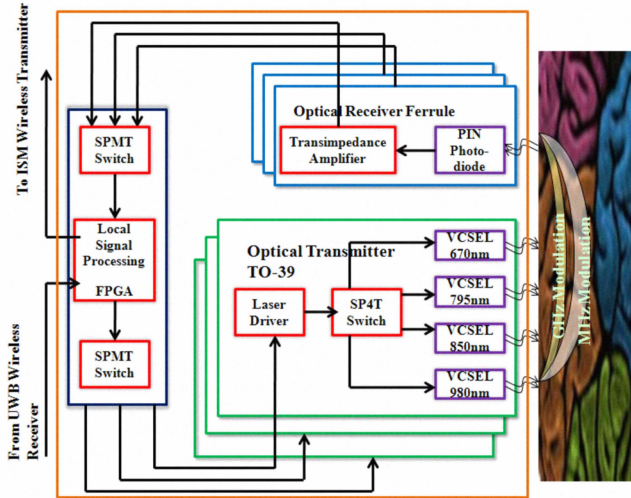


Fig. 2. Block diagram of fNIR brain imaging system using custom designed optical transmitter implemented in low profile TO-39 cans and optical receiver ferrules. Custom and commercial RFIC chips are used.

### III. HARDWARE IMPLEMENTATION

**Optical Transmitter Design:** To avoid high diffraction angles of edge emitting lasers, vertical cavity semiconductor lasers (VCSEL) are employed as optical source. Optical transmitter board consists of tri-wavelength VCSELs mounted in a TO-39 can combined with a single-pole triple through (SP3T) switch (Hittite HMC194). High-speed modulated output light is obtained by careful selection of VCSEL. The laser diodes from Vixar operating at three wavelengths of 685nm, 780nm and 850nm are characterized and fitted to an equivalent circuit model as shown in Fig. 3. The leftmost stage represents the parasitic of the package leads, followed by the inductance and capacitance of the wire bonds of the package. The intrinsic VCSEL is modeled by a series access resistance of the VCSEL in shunt with a nonlinear P-N junction capacitance  $C_j$

and resistance  $R_j$ . A network analyzer with built in Bias-Tee, calibrated to the end of the microstrip line was used to measure the reflection ( $S_{11}$ ) coefficient as a function of frequency and laser bias current. The measured VCSEL  $S_{11}$  is fitted to this equivalent circuit model, for a bias current of 9mA. The extracted values of the circuit elements are used to match the impedance measurements for the design of laser driver. These results are summarized in Table I.

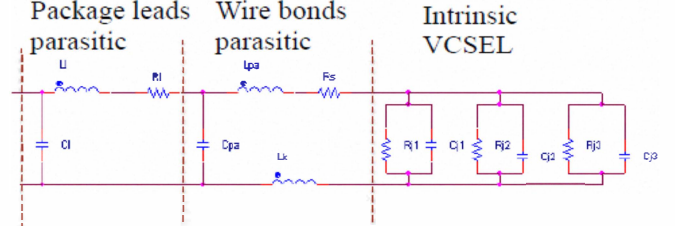


Fig. 3. Equivalent circuit model of a high-power VCSEL.

TABLE I EXTRACTED CIRCUIT COMPONENTS OF TRI-WAVELENGTH HIGH-POWER VCSEL

Parameter	685nm	780nm	850nm
$R_{j1}$	59.99 $\Omega$	24.23 $\Omega$	50 $\Omega$
$R_{j2}$	59.99 $\Omega$	20.66 $\Omega$	50 $\Omega$
$R_{j3}$	59.99 $\Omega$	24.40 $\Omega$	50 $\Omega$
$C_{j1}$	3.81pF	2.11pF	1.45pF
$C_{j2}$	3.87 pF	3.26pF	2.13pF
$C_{j3}$	3.85 pF	2.02pF	5.95 pF
$R_s$	58.26 $\Omega$	59.98 $\Omega$	64.25 $\Omega$
$C_{pa}$	0.12 pF	0.36pF	1.14 pF
$L_{pa}$	2.13nH	2.27nH	1.23nH
$R_l$	4.99 $\Omega$	2.22 $\Omega$	4.35 $\Omega$
$L_l$	1.44 nH	0.31 nH	8.67 nH
$C_l$	1.01pF	0.90pF	1.16pF

Based on the extracted static and dynamic model of VCSEL, a low power consuming active laser driver is designed with a flat frequency response 30-1000MHz. The custom IC is designed using IBM 90nm CMOS and includes SP4T switch and fixed RF drive current with adjustable DC bias current for each VCSEL to maximize current swing.

**Optical Receiver Design:** The diffused photons in brain matter are collected by 0.47 pitch GRIN lens and focused on the PIN photodiode of the optical receiver. The optical receiver is realized using an optical fiber connector ferrule with 2mm diameter GRIN rod. Standard graded index profile of lens is used for performance comparison of GRIN lens against the large diameter optical fibers using commercial CAD tool (OSLO program). The coupling efficiency of plastic fibers is between 17% (250 $\mu$ m in diameter) and 30% (1000 $\mu$ m in diameter) while for the GRIN lens coupling efficiency greater than 99% is measured. Thus GRIN lens gives us better focusing and light collection efficiency capability than even large plastic fibers.

The PIN photodiode is integrated with a transimpedance amplifier (TZA) to provide required gain without use of APD as optical detector. Even though APD provides a higher sensitivity than PIN photodiode, but due to its high reverse voltage requirements of over 100V, it could potentially lead to

electric shock of patient under test. To compensate for a lower internal gain of PIN photodiode, a TZA chip is designed using a broadband common-gate feedforward topology [6]. The trans-impedance gain of the TZA is the ratio of the output voltage to the input current and TZA gain of 58dB $\Omega$  is predicted up to 1000MHz using 90nm IBM CMOS process. The noise contribution of the TZA is characterized by the input referred noise current; the output noise voltage is related to input noise current by the trans-impedance gain  $Z_T$ . When CMOS transistors operate at radio frequencies, the random potential fluctuations in the channel resulting in the channel noise will be coupled to the gate terminal through the gate-oxide capacitance and cause the induced gate noise, which is usually correlated with the channel noise.

#### IV. OPTICAL LINK PERFORMANCE IN SOLID BRAIN PHANTOM AND PARAMETER EXTRACTION CHALLENGE

Signal to noise ratio (SNR) of free-space optical link through brain is predicted using optical insertion loss and phase calculated from Diffusion equation [1]. The absorption and scattering parameters in skull, CSF, and cortex [7] for different wavelengths are employed. SNR performance of PIN and APD based optical receivers are compared in Fig. 4 for 30kHz receiver bandwidth. Overall direct modulation link performance is product of optical transmitter & receiver gains and the square of the link current transfer function [8]. Optical Link Gain for the optical receivers using PIN with TZA is similar to APD with TZA without high voltage requirements of APD. Over the frequency range of 30-1000MHz, the predicted SNR is 20dB and higher for CSF and 60dB and higher for Cortex.

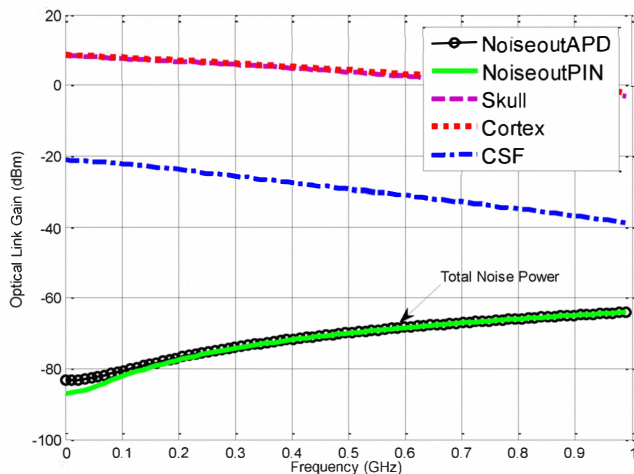


Fig. 4. Predicted Optical Link Gain versus frequency for DP-NIR waves through brain matters with 2cm separation between optical transmitter and APD and PIN-photodiode based optical receivers.

Potentially low SNR over broadband in diffused media could introduce substantial extraction errors in single frequency extraction. Due to slow variation of biological parameters, data update rate of about 1 second is considered, which is compatible with about 1ms frequency sweep rate and provides up to 1000 temporal averaging of data at each frequency. When broadband frequency sweep of 30-1000MHz with 1024 data points are considered, an incremental frequency step of 1MHz is attained with chirp

rate of GHz/ms, which corresponds to a realistic PLL locking time of about 1 $\mu$ s. A spectral averaging over 50 MHz wide bandwidth is also performed, which corresponds to about 20 frequency chunks over 1000MHz bandwidth. The compressed data provides a single value of amplitude and phase of 50 data points that are time averaged over 1 ms. When 12 bits of differential amplitude for in-phase (I) and quadrature (Q) channels are considered, it leads to an effective 8bits resolution of phase (about 1 $^\circ$  resolution). Analog to digital convertors (ADC) with 100MSPS with 12bit of differential signals is sufficient to provide the compressed 30-1000MHz received optical signals with full dynamic range of up to 75dB. The fundamental limitations in effective bits of resolution are the excessive optical link loss and the limited SNR. Since amplitude information is primarily related to absorption parameters and phase information is related to scattering parameter, extractions of absorption and scattering parameters at various wavelengths could quantify blood (650nm, 780nm, and 850nm) and water content (980nm) volume and fraction of oxy- (780nm and 850nm) and deoxy (650nm and 780nm) hemoglobin. Broad frequency data provides meaningful information of multi-layer tissue structure and provides opportunity for topographic imaging of inhomogeneous brain layers.

#### V. SYSTEM CONTROL AND WIRELESS DATA THROUGHPUT

A completely mobile and field deployable unit requires a broadband and low power consuming wireless system to communicate between the sensor and the remote monitoring device. In addition, a relatively low level signal processing function has to be achieved at the helmet mounted electronics to reduce the extremely high raw information throughput. The received signals over 30-1000MHz from optical receivers are processed locally to significantly reduce Tb/s raw data throughput to processed data rates of Mb/s [9].

Fig. 5 depicts detailed block diagram of wireless transmitter (ISM Transmitter) and receiver (UWB) chips to be used in conjunction with the 18 optical transmitters and 22 optical receivers. The fNIR sensors are strategically located on head with separation of about 2cm between the 18 optical transmitters and 22 optical receivers to perform brain imaging [10]. A broadband low weight, low size fractal antenna is selected from Fractus Inc and used for wireless transmission of the UWB signal, where a directivity gain of about 3dB is measured in both azimuth and elevation planes.

The path loss expected for transmitting wireless signal over a distance of 3m is expected to be around 50dB for an estimated path loss exponent of  $n = 2.2$  for indoor communications at 5GHz. To overcome this loss, a gain of around 25dB is required at the wireless transmitter and receiver. Low power consuming custom designed Gilbert Cell Mixer, Low Noise Amplifier and Drive Amplifier is designed using the IBM 90nm CMOS foundry parameters. Due to the complete untethered nature of the device, power consumption is a major challenge that needs to be addressed. The bandwidth requirements for each component and its



related gain/noise figure and power consumption specifications are tabulated in Table II. The first block of the receiver after the antenna is the LNA, where the overall receiver noise temperature characteristics are being established. To overcome the path loss, at least 40dB of gain is required with minimum power consumption. The designed LNA comprises of a Class A amplifier followed by a series of Class B push pull amplifiers. At 5GHz, the overall simulated gain of 32dB with a noise figure of 1.5dB and total power consumption of 25mW. For the data transmission from the monitor to sensor, we will be using custom designed wireless transmitter and receiver using 90nm CMOS technology from IBM. For the data transmission from sensor to monitor, we need a medium data rate wireless chip (e.g.a commercially available WSR601 chip from Wisair), which has a max data transmission rate of 480Mbps [11].

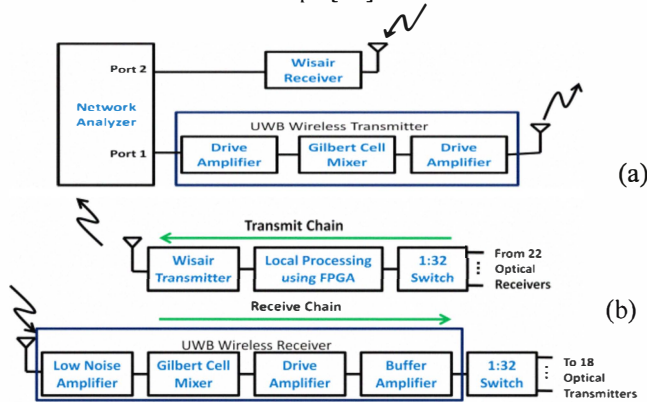


Fig. 5. Block diagram showing the structure of wireless transmitter and receiver at (a) remote monitor unit and (b) untethered helmet mounted sensor unit. The sensor unit has local signal processing performed using an FPGA. Commercial Wisair chip is used for medium data transmission of 50Mb/s.

For up- (down-) conversion between IF (RF) signals and RF (IF), a differential Gilbert Cell Mixer design topology is considered. Low Power consuming CMOS Gilbert Cell Mixer has been designed for the IF freq of 200MHz and RF frequency of 4.7GHz. The mixer has a gain of 7dB with total power consumption of 8mW using LO signal of -3dBm. The transistors performing the mixing between the RF signal and LO signal are biased at  $V_{gs} = 0.5V$  and  $V_{ds} = 0.5V$ .

Due to local signal processing performed at the sensor unit, the bandwidth needed for transmitting this information reduces to 200MHz and data throughput is 25.6Mbps. The expected SNR at the output of the optical receiver currently is only 30dB, which results in 5-bit ADC resolution. High speed, low power consuming ADC from Analog Devices can be used for conversion from analog to digital domain. Virtex 6 FPGA from Xilinx could perform the local signal processing functionality. Power consumption of this chip is around 500mW and is the main power consuming device in the helmet mounted battery operated fNIR system. The total power consumption in this system is fixed to be restricted to about 1W, which with a 2000mAh battery operating at 1.5V permits a total battery life of around hour and half, without any energy regeneration or harvesting requirements.

TABLE II SYSTEM LEVEL SPECIFICATION FOR CUSTOM DESIGNED UWB WIRELESS COMMUNICATIONS

Component	Operating Freq	Gain / NF	Power
LNA	4.5 – 5.5 GHz	30dB/1dB	<20mW
GCM	RF = 4.5-5.5GHz LO = 4.5GHz	Gain = 1dB	<5mW
RF Amp.	4.5 – 5.5 GHz	Gain = 10dB	<20mW
IF Amp.	30-1000MHz	Gain = 10dB	<20mW

## VI. CONCLUSION

Design and realization challenges of a broadband fNIR system for functional brain imaging are discussed, where extraction inaccuracy of narrowband systems and physical restrictions of fiberoptic based systems are overcome. Multi-wavelength VCSEL mounted in TO-39 can are characterized; using IBM 90nm CMOS foundry parameters and the equivalent circuit, design of laser driver circuits and low profile optical receiver are achieved. Design specifications meeting low power consumption are discussed for a helmet mounted system of real time TBI monitoring.

## ACKNOWLEDGMENT

This research is partly supported by the Center for Neuroscience and Regenerative Medicine (CNRM), and the Intramural Research Program (IRP) of Eunice Shriver National Institute of Child Health and Human Development (NICHD) of the National Institutes of Health.

## REFERENCES

- [1] Afshin S. Daryoush, "RF and Microwave Photonics in Biomedical Applications," Chapter 13 of *Microwave Photonics*, Stavros Iezekiel, Ed, Wiley (UK).
- [2] Yoko Hoshi, "Functional near-infrared optical imaging: Utility and limitations in human brain mapping," *Psychophys.*, 40 (4), p. 511.
- [3] <http://www.hondanews.com/categories/1097/releases/4975>
- [4] C. Mu *et al*, "Multi-wavelength NIR system for spectroscopy of biomedical tissues", IEEE Microwave Photonics proceeding, pp. 275 – 278, MWP 2003, Budapest, Hungary.
- [5] K. Manseta *et al*, "Development Challenges of Brain Functional Monitoring using Untethered Broadband Frequency Modulated fNIR System," IEEE Microwave Photonics proceeding, pp. 295 – 299, MWP 2010, Montreal, Canada.
- [6] C. Kromer, G. Sialm, T. Morf, M. L. Schmatz, F. Ellinger, D. Erni, H. Jackel, "A low-power 20GHz 52-dB Transimpedance Amplifier in 80-nm CMOS," IEEE Journal of Solid-State Circuits, Vol. 39, No. 6, June 2004 885.
- [7] F. Bevilacqua, D. Piguet, P. Marquet, J.D. Gross, B.J. Tromberg, C. Depeursinge, "In Vivo Local Determination of Tissue Optical Properties: Applications to Human Brain", Appl. Opt., 38 (22), pp. 4939-4950 (1999).
- [8] A. Daryoush, E. Ackerman, N. Samant, S. Wanuga and D. Kasemset, "Interfaces for high-speed Fiber-optic Links: Analysis and Experiments," IEEE Transactions on Microwave Theory and Techniques, vol. 39, no.12, December 1991.
- [9] A.M. Khwaja *et al*, "UWB Wireless Link Design and Implementation Challenges in Broadband Frequency Modulated fNIR Biomedical," IEEE Radio and Wireless Symposium, Jan. 2011, Phoenix, Az.
- [10] Y. Zhan *et al*, "Application of Subject Specific Models for Mapping Brain Function with Diffuse Optical Tomography", Biomedical Optics Topical Meeting on CD-ROM, The Optical Society of America, Washington, DC, April 11-14, (2010).
- [11] <http://www.wisair.com/wsr601>.